Journal of the European Ceramic Society **13** (1994) 229–237

Aluminium Nitride Ceramics with High Thermal Conductivity from Gas-Phase Synthesized Powders

Peter Greil,* Michael Kulig,† Dachamir Hotza

Technische Universität Hamburg-Harburg, Arbeitsbereich Technische Keramik, Denickestr. 15, D-2100 Hamburg 90, Germany

&

Horst Lange, Robert Tischtau

Bayer AG, Geschäftsbereich Pigmente und Keramik, D-4150 Krefeld-Uerdingen, Germany

(Received 6 August 1993; revised version received 15 October 1993; accepted 12 November 1993)

Abstract

Aluminium nitride powder was synthesized via a high temperature gas phase reaction process of aluminium trichloride with ammonia in flowing nitrogen atmosphere in a graphite reactor at 1600–1800 °C. After purification of the reaction product by sublimation of ammonium chloride at 900–1100 °C and calcination at 1500–1700 °C in nitrogen atmosphere a high-purity aluminium nitride powder with low residual chlorine (< 0.2 wt%) and oxygen (0.85 wt%) content and a specific surface area of 7.5 m² g was obtained. The powder was doped with various amounts of CaF_2 and sintered to full density at 1800 °C in boron nitride crucibles. Thermal conductivity after sintering reached 120 W/mK and could be increased up to 220 W/mK by 16 h annealing at 1850 °C in reducing atmosphere.

Aluminiumnitridpulver wurde über einen Hochtemperaturgasphasensyntheseprozeß von Aluminiumtrichlorid mit Ammoniak in fließender N_2-Atmosphäre bei 1600–1800 °C in einem Graphitreaktor hergestellt. Nach Reinigung des Reaktionsproduktes durch Sublimation von Ammoniumchlorid bei 900–1100 °C und Calcinierung bei 1500–1700 °C in N_2-Atmosphäre wurde ein hochreines Aluminiumnitridpulver mit einem niedrigen Restchlor (< 0.2 Masse%) und Sauerstoffgehalt (0.85 Masse%) sowie einer spezifischen Oberfläche von 7.5 m² g erhalten. Das Pulver wurde mit unterschiedlichen Gehalten von CaF_2 dotiert und in BN-Tiegeln bei 1800 °C zu vollständiger Dichte gesintert. Die Wärmeleitfähigkeit erreichte nach dem Sintern 120 W/mK und konnte durch 16 h Auslagerung in reduzierender Atmosphäre bei 1850 °C auf 220 W/mK gesteigert werden.

On a synthétisé de la poudre de nitrure d'aluminium par réaction en phase gazeuse à haute température de trichlorure d'aluminium avec de l'ammoniac, sous flux d'azote dans un réacteur graphite à 1600–1800 °C. Après avoir purifié le produit de la réaction en subliment le chlorure d'ammonium à 900–1100 °C et en le calcinant à 1500–1700 °C sous azote, on obtient une poudre de nitrure d'aluminium très pure, contenant peu de chlore résiduel (< 0.2% pd.) et peu d'oxygène (0.85% pd.) et ayant une spécifique de 7.5 m² g. On a dopé la poudre avec des quantités différentes de CaF_2, puis on l'a frittée jusqu'à 100% de la densité théorique à 1800 °C dans des creusets en nitrure de bore. La conductivité thermique après frittage peut atteindre 120 W/mK et peut être améliorée jusqu'à 220 W/mK par un recuit de 16 h à 1850 °C, en atmosphère réductrice.

1 Introduction

Aluminium nitride ceramics of high thermal conductivity (κ = 150–250 W/mK) and electrical resistivity (ρ > 10^{14} Ωm) at room temperature (RT) are of increasing interest for applications in microelectronic and electromechanical devices.[1] Aluminium nitride ceramics, for example, have been used

* Present address: Universität Erlangen-Nürnberg, Institut für Werkstoffwissenschaften, Martensstr. 5, D-91058 Erlangen, Germany.

† Present address: Siemens AG, ZFE, D-8000 München 83, Germany.

Journal of the European Ceramic Society 0955-2219/94/$7.00

commercially for packaging, hybrid substrates and multichip modules,[2,3] as heat sinks for thyristor modules and submount substrates for laser and light emitting diodes.[4] The high thermal conductivity is one of the key properties of aluminium nitride ceramics which are characterized by low density (3.26 g cm^{-3}), high hardness (H_v ~ 1500 GPa) and good mechanical strength (300–400 MPa).[5] Under triaxial loading conditions AlN was reported to undergo a brittle to ductile transition at ~ 550 MPa which gives rise to considerable plasticity during dynamic compaction.[5] Other properties of potential interest include chemical inertness towards metallic melts, a thermal expansion coefficient close to that of silicon ($\alpha \sim 4.4 \cdot 10^{-6}$ K from RT to 400 °C), semiconductivity of doped aluminium nitride with a large band gap energy ($W_g \sim 6.2$ eV at RT), optical translucency and high optical transmittance in the infrared region ($\lambda \sim 6\ \mu$m), low dielectric loss ($\tan\delta \sim 3 \cdot 10^{-4}$ at 1 MHz) and piezoelectricity.[2]

Sintered products of extremely low ionic impurity content (< 0.2 wt% of oxygen and < 0.02 wt% of metallic impurities (Si, Fe, Mg)) and an average grain size ranging from 10 to 15 μm are required to achieve a thermal conductivity value above 200 W/mK at room temperature in polycrystalline aluminium nitride (theoretical value in single crystal 320 W/mK).[6–11] With increasing substitution of oxygen atoms on the nitrogen sites in the wurtzite structure aluminium vacancies have to be formed to maintain charge balance.[10]

$$AlN + x\ Al_2O_3 \rightarrow Al_{1-1.5x}N_{1-x}(O_N)_x(V_{Al})'''_x$$

and the topology of the primary defect-type changes from isolated clusters to two dimensional extended inversion domain boundaries.[12–15] The large localized mass differences introduced by the aluminium deficiency lead to considerable anharmonicity within the lattice which leads to increased phonon scattering and causes a dramatic reduction in the thermal conductivity. It is evident that a high thermal conductivity can only be achieved if the impurity content in the AlN crystal lattice can be kept low in the starting powder or can be reduced by appropriate processing steps.

The chemical composition and grain boundary microstructure of polycrystalline aluminium nitride materials can be tailored in a wide range by controlling the high temperature reactions which take place during sintering and annealing in reducing atmosphere. Alkaline-earth metal as well as yttrium and rare-earth metal compounds are used for sintering of aluminium nitride at 1500–2000 °C in nitrogen atmosphere.[2,16] These dopants react with an amorphous oxide film on the AlN particles having a typical depth of around 0.4–1.2 μm[8] to form a liquid phase, which promotes densification by particle rearrangement and solution-precipitation upon sintering, as well as grain growth during high temperature annealing.[9] The oxygen content in the sintered AlN can be significantly reduced by carbothermal reduction of the sintered material during annealing in a carbon containing atmosphere at 1800–2000 °C.[11,17] Due to the reduction of the oxygen content below 0.1 wt% thermal conductivity of an Y_2O_3 doped AlN could be drastically increased, e.g. up to 266 W/mK after 24 h annealing at 1900 °C.[17]

Aluminium nitride powders of high sintering activity are required in order to reduce the amount of secondary phases and the duration of high temperature treatment. Powders with particle sizes less than 1 μm which are mainly produced by direct nitridation of aluminium powder below 700 °C or carbothermal nitridation of fine alumina powder in nitrogen atmosphere above 1000 °C[1] are readily available. While the powders from nitridation of metallic aluminium usually have to be milled to attain a high sintering activity, the powders produced by carbothermal reduction often contain a significant amount of excessive carbon which has to be removed in a separate processing step. A variety of alternative synthesis techniques such as direct nitridation of alumina by ammoniac gas,[18] thermal decomposition of halogenides, amides or alkyl compounds of aluminium in nitrogen or ammonia at temperatures of 500–1300 °C[19] have been developed on a laboratory scale. Ultrafine powders with particle sizes less than 50 nm were produced by reacting Al with NH_3 in an electric arc plasma furnace.[20] Powders of high chemical purity could also be obtained via thermal conversion of electrolytically formed polyiminoalane at 850 °C[21] or nitridation of Li doped aluminium melt at 1000 °C.[22,23]

In this paper the synthesis of aluminium nitride powder using a high temperature gas phase reaction process was examined. The powder was doped with calcium difluoride as non oxidic sintering aid in alcoholic suspension. Thermal conductivity of the sintered and annealed material was measured and correlated to the microstructure development during high temperature treatment. Characteristic property differences of the gas phase synthesized AlN powder compared to powders produced by other techniques will be outlined and the great potential of this powder for the fabrication of AlN ceramics with low impurity content and high thermal conductivity will be demonstrated.

2 Experimental Procedure

AlN was prepared by gas phase reaction of $AlCl_3$ with NH_3 in a graphite tube reactor at 1600–1800 °C

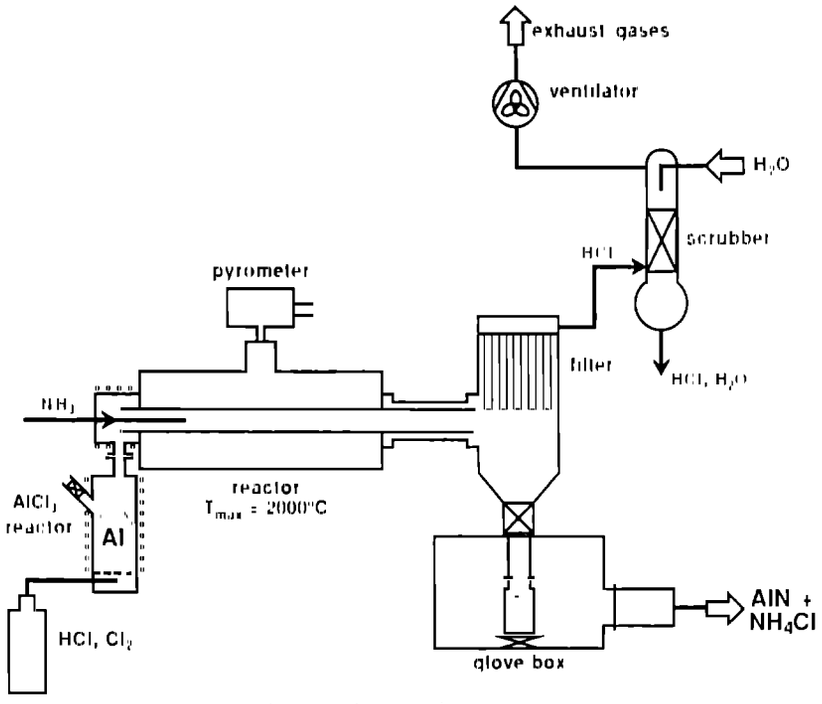

Fig. 1 Flow chart of the gas phase reactor system

in flowing N_2 atmosphere according to

$$AlCl_3 + NH_3 \rightarrow AlN + 3HCl \qquad (1)$$

Figure 1 shows the flow chart of the graphite reactor system. $AlCl_3$ was formed *in situ* by reaction of high purity aluminium foil (purity 99.95%, Merck, Darmstadt, Germany) with HCl gas in a quartz tube reactor and supplied to the AlN reactor with an accuracy of ± 2 vol%. A stoichiometric ratio of $AlCl_3$ to NH_3 was adjusted in the nitrogen gas stream. Typical reaction conditions are listed in Table 1.

The reaction products e.g. AlN, $AlCl_3 \cdot xNH_3$ adducts and NH_4Cl were collected by a filter system in inert gas atmosphere. $AlCl_3 \cdot xNH_3$ and NH_4Cl were removed from the reaction product by sublimation at 950°C in N_2 atmosphere followed by a calcination treatment at 1600°C in N_2 for 2 h. Agglomerates were crushed by milling the powders in a jet mill in N_2 atmosphere. The specific surface area of the powder was determined according to the BET method (Quantasorb, Micromeritics, Norcross, USA) and the grain size distribution was measured in diluted powder suspensions in isopropanol using laser granulometry (Mastersizer, Malvern Instruments Ltd, Worcestershire, UK). Chemical composition of the powders was analysed according to various procedures. N, O and C contents were determined via the thermal extraction method (ON- and CS-Mat analyzers, Strohlein, Kaarst, Germany). Si content was analysed by photometry (Photometer 75, Perkin Elmer, Überlingen, Germany) and Cl content was measured by potentiometric titration (Potentiograph, Metrohm, Essen, Germany). Metallic impurities were determined by an ICP emission spectral analyser (Instruments SA, Paris, France).

Table 1 Typical reaction conditions for high temperature gas phase synthesis of AlN powder

Reaction temperature	1600–1800°C
$AlCl_3$ feed rate	2–6 mol/h
NH_3 flow rate	3–18 mol/h
N_2 flow rate	700–1000 litres/h
Total gas flow rate (N_2 + NH_3)	800–1500 litres/h

Powder processing was carried out in N_2 filled glove boxes to minimize oxygen pick up due to hydrolysis when exposed to air. CaF_2 (Merck, Darmstadt, Germany) was used as the sintering aid to prepare specimens containing 2.8 wt% CaF_2. The CaF_2 powder was mechanically blended with AlN by high shear milling in dried ethanol. The powder mixture was dried in a rotary evaporator under reduced pressure and finally sieved.

The powder mixtures were isostatically pressed into pellets of 10 mm in height and diameter at 600 MPa pressure. Packing density of the green specimens attained 55% of the theoretical density. The green compacts were sintered in closed BN crucibles at 1800°C in N_2 atmosphere for 3 h in a graphite heated tube furnace (Thermal Technology Inc., Santa Barbara, CA, USA). A linear heating rate of 15°C/min was applied and linear dimensional change was recorded by a differential dilatometer system (Ingenieurburo Vakuumtechnik, Hamburg, Germany). After sintering, the final density was measured by the liquid displacement method in toluol. The sintered samples were annealed at 1850°C for different periods up to 16 h in nitrogen atmosphere. Due to the very low oxygen partial

pressure in the carbon-heated furnace the oxygen content of the sintered specimens can be significantly reduced by carbothermal reduction and evaporation of gaseous reaction products during annealing.

AlN substrates were prepared by tape casting, laminating, and sintering. AlN slips containing 30 vol% of AlN powder in a mixture of methylethyl ketone and ethanol was mixed with the appropriate amounts of dispersant (phosphorous acid ester), binder (polyvinylbutyral) and plastifier (dibutylphthalate and poly(ethylene glycol)), homogenized for 16 h, degassed and subsequently cast onto glass substrates using two doctor blades. Laminates with a thickness of 1 mm were formed by stacking 20 layers of the tape and pressing at 110°C at 50 MPa pressure. After dewaxing at 400°C for 12 h in air the laminates were pressureless sintered at 1850°C for 2 h.

Thermodynamic calculations using the microcomputer program Equitherm (VCH Verlagsgesellschaft, Weinheim, Germany) were carried out in order to estimate the magnitude of partial pressures resulting from the reaction of the powder constituents during sintering and subsequent annealing in reducing atmosphere. Thermodynamic data of relevant condensed and gas phase species were taken from Ref. 24. Based on the principle of minimum Gibbs free energy, the program calculates phase equilibria compositions (condensed and gaseous phases) for a given set of variables of state, i.e. system composition, temperature and pressure. The results are presented as partial pressure diagrams versus temperature or carbon activity in the annealing atmosphere, respectively.

Crystalline phase composition of the powder and sintered products was examined by XRD (PW 1729, Philips, Eindhoven, Netherlands) using monochromated CuK_α radiation. The microstructure of fractured surfaces of the sintered and annealed specimens was analysed in a 200 kV TEM (2000 FX, JEOL Ltd, Tokyo, Japan) and fracture surfaces were examined by SEM. Thin foils for TEM were prepared by dimpling and ion milling according to the standard procedures.

Thermal diffusivity γ was measured at room temperature according to the flash method.[25] A high power photo flash system was used to generate the heat pulse on the specimen surface. Discs with a diameter of 10 mm and a thickness of 4 mm were coated on the front side with a thin layer of carbon to ensure uniform absorption of the flash energy at the sample surface. Temperature variation with time was measured using a Cu–Ni thermocouple which was sputtered on the rear side of the samples. From the thermal diffusivity γ thermal conductivity κ was calculated ($\kappa = c_p \rho \gamma$) by taking $c_p = 0{\cdot}76$ for the heat capacity and the density ρ of the samples.

Table 2. Typical composition of the gas phase synthesized AlN powder (in wt%)

Al	64·5	Si	0·017
N	32·6	Fe	0·007
O	0·85	Ni	0·0002
C	0·078	Cr + Ca + Mg	0·008
Cl	0·2		
S_V (m^2 g)	7·5	d_{50} (μm)	0·4

3 Results

3.1 Powder synthesis and processing

The gas phase synthesized AlN powder is characterized by a low impurity content and a specific surface area of 7·5 m^2 g. An oxygen content of 0·85 wt% and a content of carbon and chlorine of less than 0·1 wt% and 0·23 wt%, respectively, was obtained, see Table 2. X ray analysis reveals AlN as the only crystalline phase. Figure 2 shows a SEM micrograph of the powder morphology. The powder particles exhibit isometric to prismatic shape, as can be expected from the hexagonal crystal structure of wurtzite type AlN. An average grain size of only 0·4 μm was determined by laser granulometry after jet milling. Figure 3 shows the grain size distribution, with 80% of the particles having a diameter within 0·2 to 1·2 μm. The uniform powder morphology and the narrow size distribution are typical for the as-grown product in contrast to crushed powders, which usually show rather irregular morphology and a broad size distribution.[4]

When exposed to an aqueous environment very fine AlN powders generally tend to be rapidly hydrolysed, due to a base catalysed reaction, resulting in a significant oxygen pick up.[26] For this reason a variety of surface chemical modifications has been developed to hydrophobize the AlN powder surface. For example, reactivity with water could be significantly reduced by surface adsorption of a monomolecular layer of a higher carboxylic

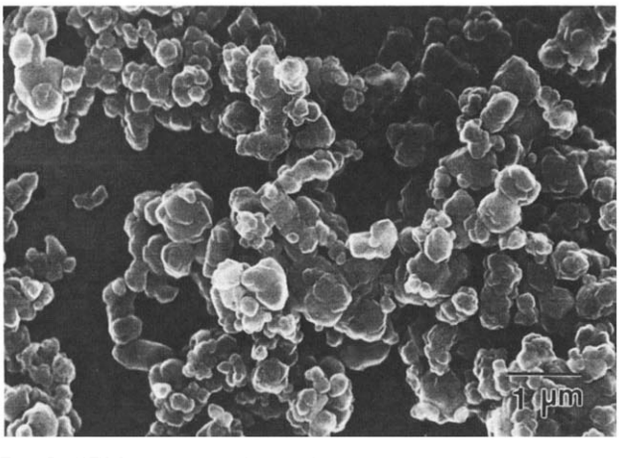

Fig. 2. SEM micrograph of the gas phase synthesized AlN powder after high energy jet milling.

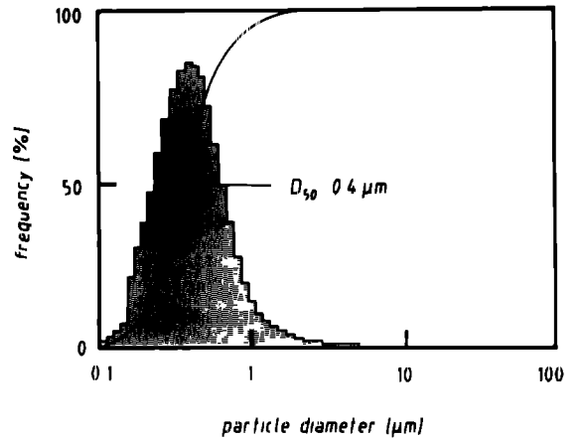

Fig. 3. Grain size distribution of the AlN powder measured by laser granulometry.

acid.[2] The organic molecule is bound to the powder surface by a covalent linkage using the hydroxyl groups present on the powder surface.[28] Stability of AlN powder versus hydrolysis can be tested by recording the variation of pH of an aqueous dispersion with time because the pH is closely related to the amount of NH_3 generated during the hydrolysis of AlN

$$AlN + 3H_2O \rightarrow Al(OH)_3 + NH_3 \quad (2)$$

$$NH_3 + H_2O \leftrightarrow [NH_4]^+ + [OH] \quad (3)$$

Figure 4 shows the variation of pH of distilled water after dispersing 0.5 vol% of as synthesized AlN powder and after coating with a long chain carboxylic acid. Surface modification was achieved by mixing the AlN powder with a solution of octadecanoic acid ($C_{18}H_{37}COOH$) in a reaction flask under rigorous stirring. While the as synthesized powder readily reacts with water, the surface treated powder remains unaffected and no pH change could be observed within the leaching period. Thus, surface modification by adsorption of suitable long chain organic molecules like suitable carboxylic acids may significantly reduce hydrophobicity of the powder which is of particular significance for

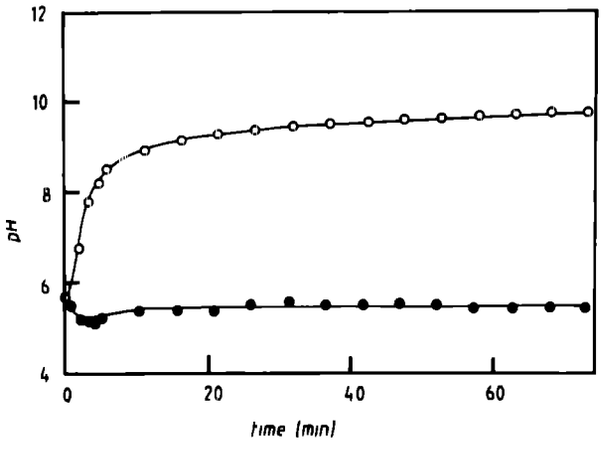

Fig. 4. pH variation of (○) as synthesized and (●) $C_{18}H_{37}COOH$ coated AlN powder in aqueous suspension (0.5 vol%).

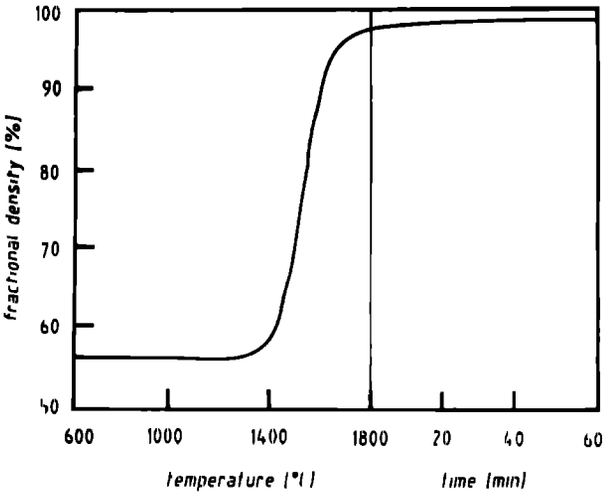

Fig. 5. Sintering behaviour of AlN doped with 4 wt% CaF_2 during heating with a constant heating rate (15 °C/min) and isothermal holding in N_2 atmosphere.

facilitated handling and storage of gas phase synthesized AlN powder with high surface area.

3.2 Sintering

Figure 5 shows the shrinkage curve of the specimen doped with 4 wt% CaF_2 during sintering with a constant heating rate of 15 °C/min to 1800 °C followed by an isothermal period. A fractional density of 95% (3.09 g cm^{-3}) was achieved at 1600 °C and a final density of >99% (3.23 g cm^{-3}) was attained after 3 h of isothermal holding. The sintered products are white in colour indicating the high purity of the AlN compact. XRD indicates the presence of small amounts of $CaAl_2O_4$ and $Ca_3Al_2O_6$ in the AlN matrix (Fig. 6(a)). The two ternary Ca aluminate phases which have melting temperatures of 1602 °C and 1539 °C respectively[29] have precipitated from the liquid phase upon cooling from the sintering temperature. The liquid phase is formed by reaction of CaF_2 with Al_2O_3 present on the AlN powder surface[30] at temperatures above 1360 °C. At this temperature a eutectic melt of approximate composition 2 CaO·Al_2O_3 is

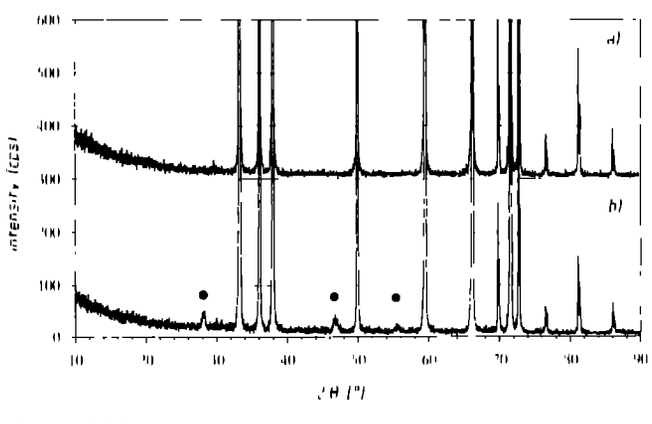

Fig. 6. XRD spectra of AlN doped with 4 wt% CaF_2: (a) after annealing at 1850 °C for 16 h in reducing atmosphere and (b) after sintering at 1800 °C for 3 h (● $CaAl_2O_4$, ○ $Ca_3Al_2O_6$).

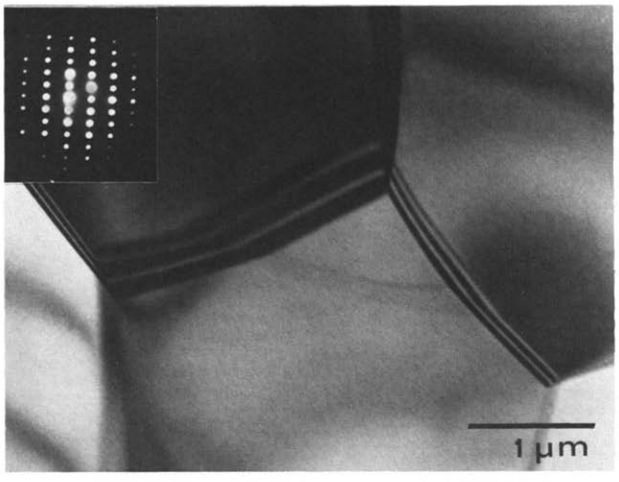

(a)

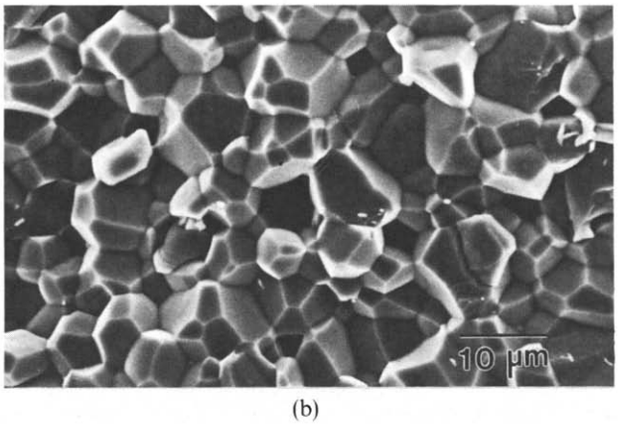

(b)

Fig. 7. Microstructure of a sintered and annealed AlN specimen doped with 4 wt% CaF_2. (a) TEM bright field micrograph of grain boundary region (b) SEM micrograph of fractured surface

formed which promotes densification via a liquid phase sintering process [4]

The sintered specimens were subsequently annealed at 1850 °C in the same furnace to reduce the amount of oxidic grain boundary phase by carbothermal reduction and evaporation of volatile reaction products. While after 6 h traces of the aluminate phases are still detectable, XRD shows no crystalline secondary phase after 16 h of thermal treatment (Fig. 6(a)). The reduction of grain boundary phase content is confirmed by TEM analysis. Figure 7(a) presents the TEM bright field micrograph of the sample with 4 wt% of CaF_2 after 16 h annealing, indicating that the grain boundaries are almost free of any secondary phase and plane boundaries of well faceted grains have been developed upon grain growth. Figure 7(b) shows the SEM micrograph of a typical microstructure on the fracture surface. The well-faceted grain morphology is associated with a predominant intergranular fracture mode. Mean grain size as determined from direct observation is approximately 10 µm.

3.3 Thermal conductivity

Figure 8 shows the thermal conductivities of the

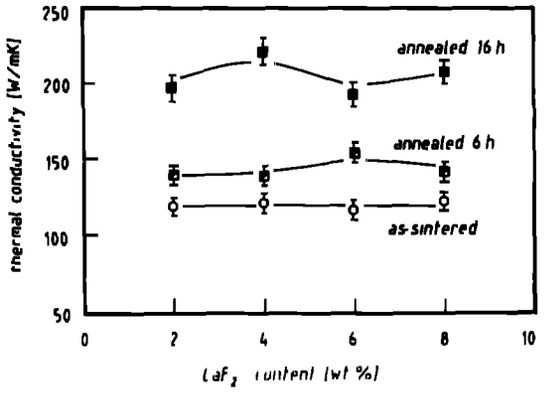

Fig. 8. Room temperature thermal conductivity of AlN as a function of CaF_2 content and thermal treatment

specimens as a function of thermal treatment and CaF_2 content. As is to be expected, the reduction of secondary phase content by annealing in reducing atmosphere resulted in a pronounced increase of thermal conductivity. For the specimen with an initial content of 4 wt% of CaF_2 thermal conductivity λ increased from 120 W/mK of the sintered specimen to 140 W/mK after 6 h and to 220 W/mK after 16 h annealing at 1850 h in an open BN crucible. With increasing CaF_2 content no significant change of thermal conductivity could be observed.

4 Discussion

AlN powder can be sintered with various additives, with Y_2O_3, CaO and rare earth oxides as the mainly used dopants [1–6]. In contrast to the powders formed by direct nitridation or carbothermal reduction-nitridation, the gas phase synthesized AlN powder exhibits significantly lower levels of thermal conductivity with oxidic sintering aids, whereas thermal conductivity values above 200 W/mK could easily be achieved with non oxide sintering aids such as CaF_2 and YF_3. Therefore

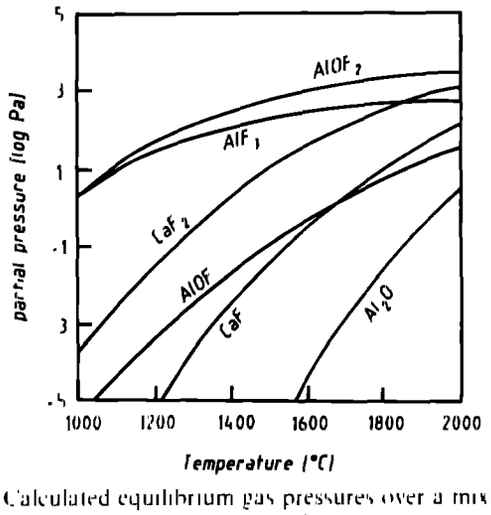

Fig. 9. Calculated equilibrium gas pressures over a mixture of CaF_2, Al_2O_3 in N_2 atmosphere (sintering)

CaF_2 was used as a sintering aid which decomposes during heating to form a low melting liquid phase in the system Ca–Al–O–N. Calculation of the gas pressures that are in equilibrium with an equimolar mixture of CaF_2 and Al_2O_3 in N_2 atmosphere (Fig. 9) shows $AlOF_{(g)}$, $AlF_{3(g)}$ and $CaF_{2(g)}$ to be the major gaseous reaction products. No residual CaF_2 could be found by XRD and TEM, suggesting the excess of CaF_2 (for an oxygen content of 0.85 wt% (= 1.81 wt% Al_2O_3) an equimolar CaF_2 content of 1.38 wt% is calculated) to be evaporated from the powder compact during high temperature sintering. Thus, the overall reaction sequence responsible for liquid phase sintering to occur during heating may be expressed, to a first approximation, by

$$12CaF_2(s) + 12Al_2O_3(s) + N_2(g) \xrightarrow{\text{sinter}} [12CaO{\cdot}6Al_2O_3{\cdot}2AlN](l) + 6AlOF_{(g)} + 4AlF_{3(g)} \quad (4)$$

with $CaAl_2O_4$ and $Ca_3Al_2O_6$ precipitating from the eutectic melt upon cooling[31]

$$[12CaO{\cdot}6Al_2O_3{\cdot}2AlN](l) \xrightarrow{\text{cooling}} 3CaAl_2O_4(s) + 3Ca_3Al_2O_6(s) + 2AlN(s) \quad (5)$$

Annealing the sintered specimens in a carbon heated furnace in nitrogen atmosphere at temperatures equal to or above the sintering temperature significantly improves thermal conductivity. From measurements of the phonon mean free path (10–30 nm at RT, which is too small to compare with the AlN grain size of 1–40 μm) it has been concluded that the oxygen dissolved in the AlN lattice determines the thermal conductivity and not the grain boundary phase.[32] The dissolved oxygen content however was shown to be strongly related to the oxygen content in the grain boundaries of sintered AlN, because the chemical reactions to improve AlN thermal conductivity by decreasing the oxygen content occur at the grain boundaries.[11] From the difference of grain boundary phase composition on the surface and in the bulk a selective carbothermal reduction and nitridation reaction of the different constituents of the grain boundary liquid was concluded.[11,33] For Y_2O_3 doped AlN, for example, the interaction with a reducing atmosphere results in the formation of AlN in the bulk, whereas YN was found to be concentrated in the surface region and weight loss was attributed mainly to the evaporation of CO.

For the case of AlN containing Ca aluminates an incongruent vaporization of the liquid phase was postulated to occur.[34] Calculation of partial pressures of gaseous reaction products in equilibrium with a liquid of a composition corresponding to $CaAl_2O_4$ at 1850°C shows CO and Ca with the highest evaporation pressures over a wide range of carbon activities in the annealing atmosphere (Fig. 10). Thus the reduction of grain boundary phase content is suggested to be dominated by the volatilization of CO and Ca from the surface according to

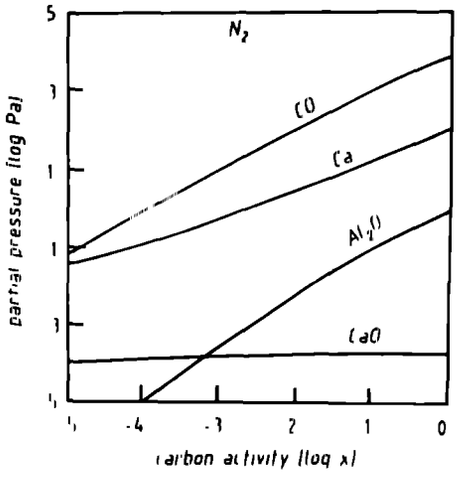

Fig. 10. Calculated equilibrium gas pressures over $CaAl_2O_4$ in N_2 atmosphere at 1850°C as a function of carbon activity (annealing in reducing atmosphere).

$$CaAl_2O_4(l) + N_2(g) + 4C(g) \rightarrow 2AlN(s) + 4CO(g) + Ca(g) \quad (6)$$

$$Ca_3Al_2O_6(l) + N_2(g) + 6C(g) \rightarrow 2AlN(s) + 6CO(g) + 3Ca(g) \quad (7)$$

resulting in a substantial increase of thermal conductivity.

The increase of thermal conductivity with annealing time (given in h) as derived from the data plotted in Fig. 8 follows a simple linear relation

$$\kappa = \kappa_0(1 + Kt) \quad (8)$$

with $\kappa_0 \approx 100$ W/mK and the time constant $K \approx 7.7$/h. Thermal conductivity of the sintered specimen κ_0 is mainly controlled by the oxygen content dissolved in the AlN lattice and by the microstructure, i.e. porosity, impurity content etc. The time constant K relates the thermal conductivity increment with the reduction of oxygen content due to evaporation of volatile grain boundary species given in eqns (6) and (7). The total amount of evaporated grain boundary material m is given by the double integral over time t and evaporation area A[35]

$$m = \sum_i \int_t \int_{A_i} \Gamma_i \, dA_i \, dt \quad (9)$$

where Γ_i is a uniform evaporation rate

$$\Gamma_i = \left[\frac{M_i}{2\pi k\bar{T}}\right]^{1/2} p_i^s \quad (10)$$

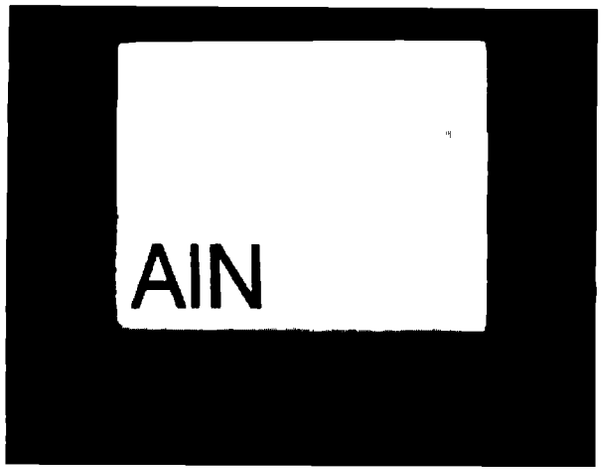

Fig. 11 Sintered AlN substrate (35 × 27 × 1 mm³) showing translucency

with p_i^t being the temperature dependent equilibrium pressures and M_i the molecular weights of evaporating species i (CO and Ca, respectively). From eqns (9) and (10) a linear increase of weight loss with time is predicted, which has been confirmed by experimental observation [11]. The slope of the linearity depends on the partial pressure and the evaporation area. For the partial pressure regimes given in Fig. 10 evaporation rates Γ_i in the range of 10^{-6}–10^{-3} g cm^{-2} s and 10^{-8}–10^{-4} g/cm^2 s are estimated for CO and Ca, respectively. Combined with the high specific surface area of the gas phase synthesized powder which provides a high evaporation area as well as fast transport of grain boundary species to the surface a rapid 'cleaning' of the material can be obtained with relative ease. Thus, the gas phase synthesized AlN powder doped with CaF_2 seems to be particularly qualified for fabrication of high purity sintered products which may achieve excellent thermal conductivity. Figure 11 shows a substrate (35 × 27 × 1 mm³) prepared from the gas phase sintered AlN powder which exhibits translucency due to its low impurity content.

5 Conclusions

High temperature synthesis of AlN by reaction of $AlCl_3$ with NH_3 in a gas phase reactor at 1800°C resulted in a powder with low impurity content and high specific surface area. Despite the high reactivity, coating of the powder with octadecanoic acid significantly reduced sensitivity to hydrolysis which facilitates handling and processing of the powder even in aqeous environment. Pressureless sintering to full density could easily be achieved utilizing common sintering additives. Compared to oxidic additives, however, non oxidic sintering aids such as CaF_2 seem to be much more effective in yielding high thermal conductivity above 200 W/mK at RT. Reduction of oxygen rich grain boundary phase content by annealing in C-containing nitrogen atmosphere is accelerated by rapid diffusion along the high grain boundary interface area and high volatility of gaseous reduction products in the system Ca–Al–N–O–C. Sintered products of low impurity content and excellent thermal conductivity were produced, demonstrating the potential of the gas phase synthesized AlN powder for applications in the field of high performance ceramics.

Acknowledgement

O. Sahling and T. Erny are acknowledged for experimental assistance. The German Ministry for Science and Technology (BMFT) is acknowledged for financial support of this work under contract no. 03M2046B9.

References

1 Foster, D., AlN and BN powders for advanced applications. *Ceram. Eng. Sci. Proc.*, **6** (1985) 1305.
2 Marchant, D. D. & Nemecek, T. E., Aluminum nitride preparation, processing and properties. *Adv. Ceram.* **26** (1989) 19.
3 Sheppard, L. M., Aluminum nitride: a versatile but challenging material. *Am. Ceram. Soc. Bull.* **69** (1990) 1801.
4 Kuramoto, N., Taniguchi, H. & Aso, I., Development of translucent aluminum nitride ceramics. *Am. Ceram. Soc. Bull.*, **68** (1989) 883.
5 Heard, H. C. & Cline, C. F., Mechanical behavior of polycrystalline BeO, Al_2O_3 and AlN at high pressures. *J. Mat. Sci.* **15** (1980) 1889.
6 Slack, G. A., Nonmetallic crystals with high thermal conductivity. *J. Phys. Solids* **34** (1973) 321.
7 Okamoto, M., Arakawa, H., Oohashi, M. & Ogihara, S., Effect of microstructure on thermal conductivity of AlN ceramics. *J. Ceram. Soc. Jpn, Int. Edn.* **97** (1989) 1486.
8 Sakai, T., Kuriyama, M., Inukai, T. & Kizima, T., Effect of the oxygen impurity on the sintering and the thermal conductivity of AlN polycrystal. *J. Ceram. Soc. Jpn, Int. Edn.* **86** (1978) 174.
9 Kuramoto, N., Taniguchi, H. & Aso, I., Sintering process of translucent AlN and effect of impurities on thermal conductivity of AlN ceramics. *J. Ceram. Soc. Jpn.* **93** (1985) 817.
10 Slack, G. A., Tanzilli, R. A., Pohl, R. O. & Vandersande, J. W., The intrinsic thermal conductivity of AlN. *J. Phys. Chem. Sol.* **48** (1987) 641.
11 Watari, K., Kawamoto, M. & Ishizaki, K., Sintering chemical reactions to increase thermal conductivity of aluminium nitride. *J. Mat. Sci.* **26** (1991) 4727.
12 Hagege, S., Ishida, Y. & Tanaka, S., TEM analysis of impurity induced microstructures in sintered aluminium nitride ceramics. *J. Ceram. Soc. Jpn, Int. Edn.* **96** (1988) 1093.
13 Youngman, R. A. & Harris, J. H., Luminescence studies of oxygen related defects in aluminium nitride. *J. Am. Ceram. Soc.* **73** (1990) 3238.
14 Pilyankevich, A. N., Britun, V. F. & Olevnik, G. S., Microstructural studies of polytype formation in oxygen containing aluminium nitride. *J. Mat. Sci.* **25** (1990) 3517.
15 Denanot, M. F. & Rabier, J., Extended defects in sintered AlN. *J. Mat. Sci.* **24** (1989) 1594.

16 Troczynski T B & Nicholson P S Effect of additives on the pressureless sintering of aluminium nitride between 1500 C and 1800 C *J Am Ceram Soc* **72** (1989) 1488
17 Ueno F & Horiguchi A, Grain boundary phase elimination and microstructure of aluminium nitride In *Euro Ceramics* Vol 1 ed P Vincenzini Elsevier London 1989 p 1383
18 Direct Nitridation of Alumina with Ammoniac Gas French Patent 2 594 109 10 February 1986
19 Brunner, S G Hohengiellen Sintern und Anwendungen von Aluminiumnitrid *Sprechsaal*, **121** (1988) 181
20 Ishizaki K Egashira T Tanaka K & Celis P B Direct production of ultrafine nitrides (Si_3N_4 and AlN) and carbides (SiC WC and TiC) powders by the arc plasma method *J Mat Sci* **24** (1989) 3503
21 Seibold M M & Russel C Thermal conversion of preceramic polyaminoalane precursors to aluminium nitride characterization of pyrolysis products *J Am Ceram Soc* **72** (1989) 1803
22 Scholz, H & Greil P Syntheses of high purity AlN by nitridation of Li doped Al melt *J Eur Ceram Soc* **6** (1990) 237
23 Haussonne J M Lostec J Bertot, J P Lostec L & Sadon S A new synthesis process for AlN *Bull Am Ceram Soc* **72**(8) (1993) 84
24 Barin I Thermochemical data of pure substances Verlag Chemie Weinheim Germany 1989
25 Enck R C Harris R D & Youngman R A, Measurement of the thermal diffusivity of translucent aluminum nitride In *Ceram Trans*, Vol 1 ed W S Young G L McVay & G E Pike American Ceramic Society Westerville OH 1988 p 214
26 Reetz I Mönch, B & Saupe, M Aluminium nitride hydrolysis *Ceram Tor Int Ber Dt Keram Ges* **69** (1992) 464
27 Egashira M Shimizu Y & Takasuhi S Chemical surface treatments of aluminium nitride powder suppressing its reactivity with water *J Mat Sci Lett* **10** (1991) 994
28 Wolfram S M & Pompe J L, Surface modification of powders with carboxylic acid *J Mat Sci Lett* **8** (1989) 667
29 Levin E M & McMurdie, H F (eds) *Phase Diagrams for Ceramists 1975* (*Suppl*) National Bureau of Standards Washington DC 1975 Fig 4308
30 Ponthieu E Grange P Delmon B Tomas L Leclercq L Bechara R & Grimblot J Proposal of a composition model for commercial AlN powders *J Eur Ceram Soc* **8** (1991) 233
31 Kurokawa Y Utsumi K & Takamizawa H Development and microstructural characterization of high thermal conductivity aluminium nitride ceramics *J Am Cer Soc* **71** (1988) 588
32 Watari K Ishizaki K & Fujikawa T Thermal conduction mechanism of aluminium nitride ceramics *J Mat Sci* **27** (1992) 2627
33 Yagi T Shimozaki K, Mizutani N Kato M & Sawada Y Migration of grain boundary phases in AlN ceramics by heating in a reducing atmosphere *J Ceram Soc Jpn Int Ed* **97** (1989) 1374
34 Odagawa T Makihara H Kamehara N & Niwa K Influence of firing gas pressure on the microstructure and thermal conductivity of AlN ceramics *J Mat Sci Lett* **9** (1990) 116
35 Maissel L I & Glang R *Handbook of Thin Film Technology* McGraw Hill Corp NY 1970